Volume 1 | Number 1 | Jan 2013 | Pages 1–100

Dalton Transactions

An international journal of inorganic chemistry
www.rsc.org/dalton

ROYAL SOCIETY OF CHEMISTRY

ROYAL SOCIETY OF CHEMISTRY

www.rsc.org/dalton

Journal Name

RSCPublishing

ARTICLE

Regulation of pore size by shifting coordination sites of ligands in two MOFs: enhancement of CO_2 uptake and selective sensing of nitrobenzene

Srinivasulu Parshamoni,‡ Jyothi Telangae‡,† and Sanjit Konar*

Two metal-organic frameworks (MOFs), namely $\{[Cd_2(sdb)_2(4\text{-}bpmh)_2(H_2O)]\}_n \cdot 2n(H_2O)$ (**1**), $\{[Cd_2(sdb)_2(3\text{-}bpmh)_2]\}_n \cdot 3n(H_2O) \cdot n(C_6H_5NO)$ (**2**), [sdb = 4,4'-Sulfonyl dibenzoic acid; 4-bpmh = N,N-bis-pyridin-4-ylmethylene-hydrazine, 3-bpmh = N,N-bis-pyridin-3-ylmethylene-hydrazine, C_6H_5NO = 3-Pyridinecarboxaldehyde] have been synthesized by the solvent diffusion technique at room temperature. Structure determination reveals that compound **1** has 2D interdigitated architectures whereas **2** is a 2-fold interwoven 3D porous network but both **1** and **2** perceives a common secondary building unit (SBU) $[Cd_2(sdb)_4(L)_4]$ [L= 4-bpmh (**1**) and 3-bpmh (**2**)]. Gas adsorption studies demonstrate that compound **2** shows high selectivity for CO_2 over CH_4 and the uptake amounts are almost double in comparison with compound **1** and both the compounds show high sensitivity for nitrobenzene via the fluorescence quenching mechanism.

Introduction

Selective carbon dioxide capture from fuel gas and natural gas has attracted much interest and became a critical issue because of global warming and the corresponding climate changes.[1] Thus, the development of new materials which show effective capture and separation of CO_2 at ambient conditions, fast CO_2 adsorption–desorption, and low energy requirement for operation and regeneration is urgently needed for some significant industrial applications such as natural gas purification. To date, covalent organic frameworks (COFs),[2] zeolite[3] and Metal organic frameworks (MOFs) have proven to be efficient materials for CO_2 capture. Among all these materials MOFs are most promising because of their permanent porosity, high surface area, large pore volume, and adjustable pore sizes.[4] In order to enhance CO_2 adsorption capacity and selectivity, various efforts have been made by incorporating functional groups such as -COOH, $-SO_3H$, and $-NH_2$ into the pores through ligand modification.[5] Furthermore, the selectivity for CO_2 adsorption can also be enhanced by mixed ligand co-ordination polymers (CPs) using polycarboxylates and N,N′ donor spacers. The role of the N,N′-donor spacers in terms of their length, flexibility, coordination ability, nature of coordination sites etc. are investigated thoroughly to see diversity both in structures as well as their properties. But, the effect of change in position of coordination site of the N,N′-donor spacers (use of bent spacers instead of straight) in the formation of networks and their gas adsorption properties has not been explored properly.

Apart from the gas adsorption, recently, more attention has been paid to the detection of explosives and other hazardous chemicals that are essential for security control and environmental safety.[6] Among the various nitroaromatics, nitrobenzene is the simplest and basic component of explosives. Additionally, nitrobenzene is a highly toxic environmental pollutant, which could be a source of serious health problems.[7] The current methods for the detection of nitro compounds by the use of sophisticated instruments are limited which are costly and not easily accessible.[8] For this purpose, some luminescent MOFs have been tested for the potential applications in detection of electron-deficient nitroaromatics by fluorescence quenching method.[9] Recently, Shi et al. reported the first case of a dual functional luminescent sensor that can quantitatively detect nitrobenzene (NB).[9c] Our group reported dual sensing property of $\{[Zn(C_{34}H_{18}O_8)_{0.5}(C_{20}N_2H_{16})_{0.5}][0.5(C_{20}N_2H_{16})2H_2O]\}_n$ MOF for the selective detection of PA and Pd^{2+}, even in presence of other competing analogues.[9d] It has been reported that in luminescent MOFs, the delocalized π-electrons of aromatic ligands increase the electrostatic interaction between the framework and the electron deficient nitroaromatics.[9e, 9f]

In this context, we have chosen two azine functionalized and pyridyl based ligands N,N-bis-pyridin-4-ylmethylene-hydrazine (4-bpmh) and N,N-bis-pyridin-3-ylmethylene-hydrazine (3-bpmh) along with a V-shaped sdb linker which lead to $\{[Cd_2(sdb)_2(4\text{-}bpmh)_2(H_2O)]\}_n \cdot 2n(H_2O)$ (1) and $\{[Cd_2(sdb)_2(3\text{-}bpmh)_2]\}_n \cdot 3n(H_2O) \cdot n(C_6H_5NO)$ (2) [sdb = 4,4'-Sulfonyl dibenzoic acid, C_6H_5NO = 3-Pyridinecarboxaldehyde] respectively (Scheme 1) and invested their gas adsorption and

Dalton Transactions Accepted Manuscript

sensing properties. The results demonstrate that compound **2** shows better CO_2 uptake at ambient conditions over compound **1** and both the compounds show high sensitivity for nitrobenzene via fluorescence quenching mechanism.
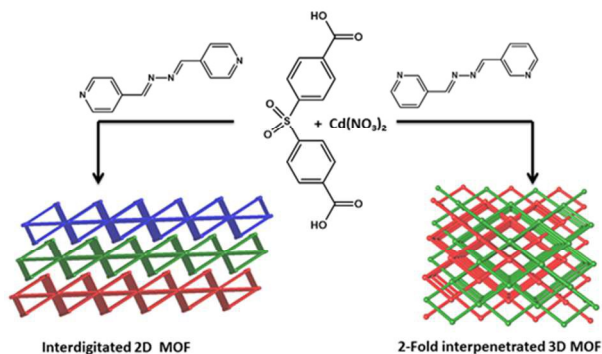
Scheme 1. Schematic view of the comparative synthesis of **1** and **2**.

Results and discussions

Synthetic Aspects

Compounds **1** and **2** were synthesized using sodium salt of 4,4'-Sulfonyl dibenzoic acid, 4-bpmh, 3-bpmh and $Cd(NO_3)_2 \cdot 4H_2O$ in 1 : 1 : 1 molar ratio through solvent diffusion technique using methanol and water (1 : 1) mixture at room temperature. Both the compounds show similar type of FT-IR spectra (Fig. S1), A broad band observed in the region 3102–3400 cm^{-1}, specifies the O–H band stretching vibrations of the guest solvent molecules (H_2O and CH_3OH). The characteristic bands for the asymmetric ($v(COO)_{asym}$) and symmetric stretching vibrations ($v(COO)_{sym}$) of the carboxylate groups appear at 1609 cm^{-1} and 1392 cm^{-1} respectively. The noted difference ($\Delta v = v(COO)_{asym}$

– $v(COO)_{sym}$ (217)) in compounds **1** and **2** may confirm the bridging mode of the carboxylate groups.[10]

Structural Description of {[Cd$_2$(sdb)$_2$(4-bpmh)$_2$(H$_2$O)]}$_n \cdot 2n(H_2O)$ (1):

Compound **1** crystallizes in triclinic system with the *P*-1 space group, and the single crystal X-ray diffraction analysis reveals that the 2D coordination framework of Cd(II) is bridged by the dicarboxylate (sdb) and linear Schiff base linker (4-bpmh). The asymmetric unit of **1**, contains two crystallographically different Cd(II) ions, two sdb, two 4-bpmh ligands and one coordinated water molecule (Fig. S2). Cd1 center is hexa-coordinated by four oxygen atoms from three different sdb ligands which are occupied in the equatorial position and two 4-bpmh linkers in the axial position resulting in a distorted octahedral geometry (Fig. S3). The Cd2 adapts distorted octahedron geometry by the contribution of three oxygen atoms from two different sdb ligands and one water molecules in the equatorial position and two nitrogen atoms from two different 3-bpmh linkers in the axial site (Fig. S4). Measured Cd-O bond lengths are in the range of 2.19(7) - 2.69(2) Å whereas Cd-N bond lengths are in the range of 2.304(9) - 2.33(1) Å. The bond angles around Cd(II) centers are in the range of 84.5(3)–179.1(3)°. In **1**, the sdb ligand displays two kinds of coordination modes to connect Cd(II) centers with two carboxylate groups, either μ-1,2 (2.11 in Harris notation) and chelating bridging modes (1.11 in Harris notation), or chelating bridging modes μ-1,1 (1.11 in Harris notation) and μ-1 (1.1 in Harris notation) (Fig. S5).[11]

It was found that each sdb connected to two crystallographically different Cd(II) ions and forming 1D zig-zag chain along the *c*-axis as shown in Fig. 1b. Similarly those linked by 4-bpmh linkers are extended in a 1D chain along the *b*-axis (Fig. S6).
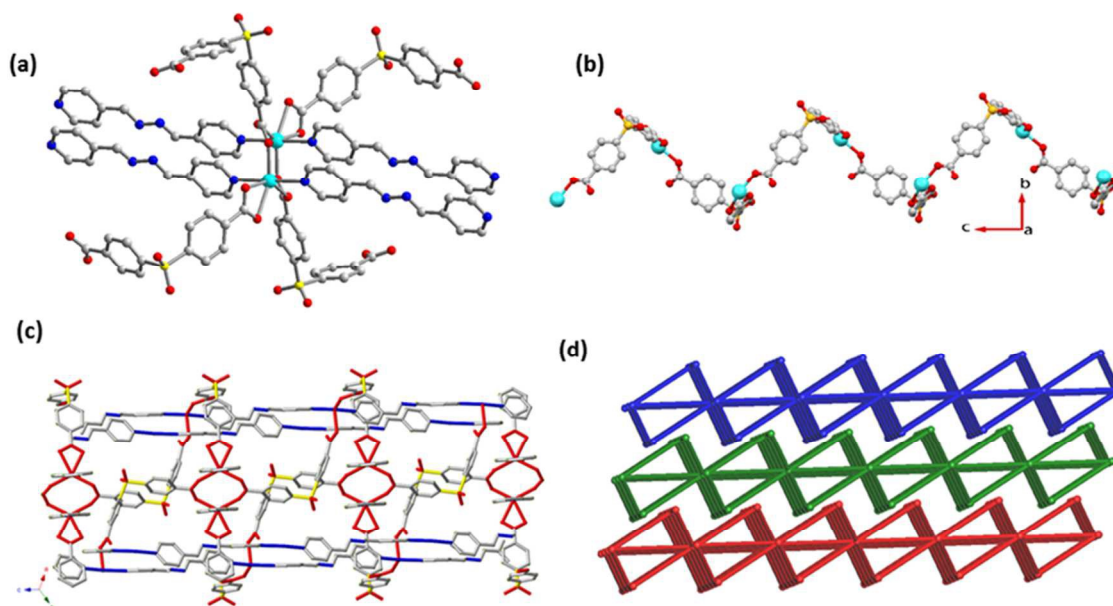

Fig. 1. (a) A view of SBU found in compound **1**. (b) Illustration of 1D chain found in **1** by sdb ligands in *c*-axis (4-bpmh linkers are omitted for clarity). (c) Illustration of 2D network along the *bc*-plane. (d)) Illustration of interdigitated 2D network with {4³.6².8}2{4⁶.6⁸.8} *ssj1* topology featuring a 6-connected binodal net.

The aforementioned two 1D chains are perpendicularly interconnected on the *bc*-plane to form a 2D sheet like structure (Fig. 1c). The parallel 2D sheets of one set are displaced with each other half the length of the grid side (Fig. 1d) and are interdigitated (also known as inclined interpenetration) with another set of parallel 2D sheets (Fig. 1d). PLATON[13] analysis reveals that compound **1** exhibit pore accessible void volume of 318.9 Å^3 out of 2735.5 Å^3 which represents 11.3 % per unit cell volume (details in SI). Topological perception of **1** reveals that, both the sdb ligands and 4-bpmh linkers are connected to two Cd(II) centers and so can be considered as a two connected node. Each Cd(II) is linked to nearby six Cd(II) centres by four sdb ligands and four 4-bpmh linkers. Therefore, the 2D interdigitated framework can be simplified as a 6-connected binodal net with a point symbol of $\{4^3.6^2.8\}2\{4^6.6^8.8\}$ exhibiting a new type topology of *ssj1* in the Reticular Chemistry Structure Resource (RCSR) database[14] (Fig. 1d and S7).

Structural Description of $\{[Cd_2(sdb)_2(3\text{-}bpmh)_2]\}_n \cdot 3n(H_2O) \cdot n(C_6H_5NO)$:

Compound **2** crystallizes in monoclinic system with a *P* 2/n space group. The asymmetric unit consists of two crystallographically different Cd (II) ions, two sdb and two 3-bpmh ligands (Fig. S8). The Cd1 adapts distorted octahedron geometry by the contribution of four oxygen atoms from three different sdb ligands, and two nitrogen atoms from two different 3-bpmh linkers (Fig. S9). The Cd2 is hepta coordinated by five oxygen atoms of three different sdb ligands and two nitrogen atoms from two different 3-bpmh linkers and results a pentagonal bi pyramidal geometry (Fig. S10). It was found that in both Cd(II) centers, the carboxylate oxygen atoms of the sdb ligands are in the equatorial positions whereas the nitrogen atoms of the 3-bpmh linkers are in the axial positions. The measured Cd-O bond lengths are in the range of 2.27(7) - 2.78(8) Å whereas Cd-N bond lengths are in the range of 2.31(8) - 2.36(9) Å. The bond angles around Cd(II) center are found in the range of 55.0(2) – 171.6(3)°.
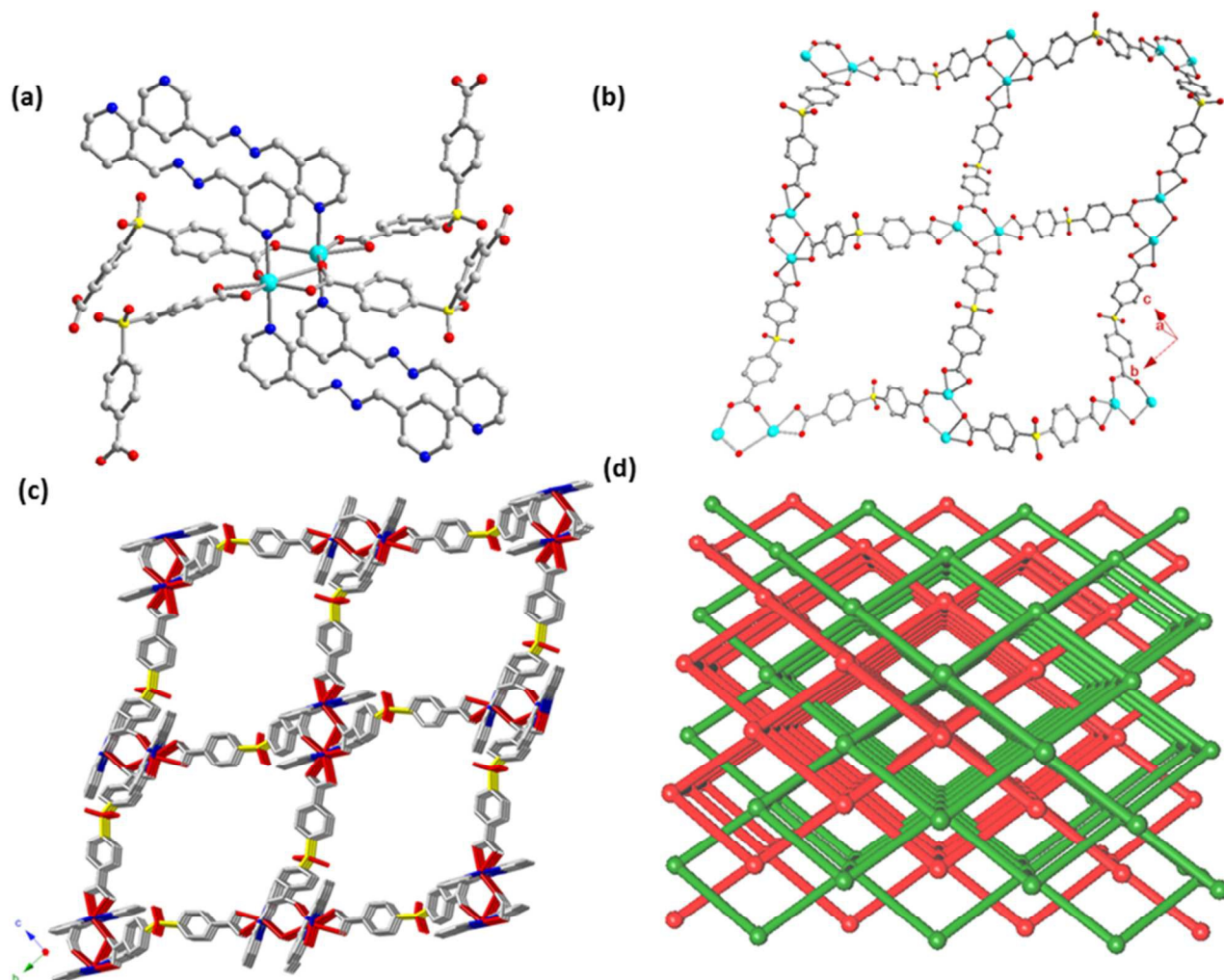

Fig. 2. (a) A view of SBU found in compound **2**. (b) Illustration of 2D layered structure found in **2** by sdb ligands in *bc*-plane (3-bpmh linkers are omitted for clarity). (c) Illustration of 3D network with one-dimensional (1D) channels along the *a*-direction (d) View of the $\{4^{12}.6^3\}$ *pcu alpha-Po primitive cubic; 6/4/c1; sqc1* topology featuring a 6-connected uninodal net.

Like **1**, in **2** also sdb ligand displays two kinds of coordination modes to connect three Cd(II) centers with two carboxylate groups, adopting either μ-1,2 (2.11 in Harris notation) and chelating bridging modes μ-1,1 (1.11 in Harris notation) or μ-1,1',2 (2.21 in Harris notation) and μ-1,2 (2.11 in Harris notation) bridging modes (Fig. S11). Compound **2** also contains a [Cd$_2$(sdb)$_4$(3-bpmh)$_4$] unit as secondary building units (SBUs) in which one Cd(II) center is μ-oxobridged and the distance between two Cd(II) centers in the SBU is 4.06(1) Å (Fig. 2a).

Like **1**, in **2** also each SBU is connected to six neighboring SBUs by sdb and 3-bpmh ligands. It was found that SBUs that are connected by only carboxylate oxygen atoms of sdb ligands arranged to form 2D layered like structure along the *bc*-plane (Fig. 2b). Whereas those linked by 3-bpmh linkers are extended only in a 1D chain (Fig. S12). Furthermore, the adjacent 2D layers are pillared by nitrogen atoms of 3-bpmh linkers along the *a*-direction to generate a porous 3D network with one-dimensional (1D) channels having cross section of 17.901(1) x 23.068(1) Å^2 (considering the distance between two Cd(II) centres bridged by sdb ligands) running along the *b*-axis (Fig. 2c). The existence of large rectangular channels along with bent shape of spacers assists interweaving of one 2D net over another to generate a 2-fold interwoven 3D network. As a result, pore size of the 1D channels is reduced (Fig.2d, Fig. S13). These channels are occupied by guest molecules. PLATON analysis revealed that compared to **1**, compound **2** exhibits large pore accessible void volume of 1713.1 Å^3 out of 6250.1 Å^3 that represents 27.4% per unit cell volume (details in SI).

Topological perception of **2** reveals that each Cd(II) is linked to nearby six Cd(II) centres by four sdb ligands and four 3-bpmh linkers. Therefore, the 3D interpenetrated porous framework can be simplified as a 6-connected uninodal net with a point symbol of {4^{12}.6^3} exhibiting a *pcu alpha-Po primitive cubic; 6/4/c1; sqc1* topology[14] (Fig. S14).

PXRD and Thermal Stabilities

In order to check the phase purity of the bulk materials, powder X-ray diffraction (PXRD) experiments were carried out on compounds **1** (Fig. S15) and **2** (Fig. S16). All major peaks in experimental PXRD of compounds **1** and **2** match well with simulated pattern from single crystal data, and that indicates equitable crystalline phase purity.

Thermogravimetric analysis (TGA) of compounds **1** and **2**, were carried out in the temperature range of 30-800 °C under the flow of N$_2$ with a heating rate of 10 °C min^{-1} (Fig. S17). Compound **1** shows a loss of 5 wt% (calc. 4.8 wt%) around 80-119 °C, which corresponds to the loss of one coordinated water molecule and two guest water molecules and the desolvated framework is stable up to 344 °C, followed by a sharp weight loss due to the decomposition of the framework. A weight loss of 13 wt% (~12 cald.%) observed in compound **2** in the range of 60-130 °C, which can be assigned to the loss of one guest 3-Pyridinecarboxaldehyde and three H$_2$O molecules

and the dehydrated framework was stable up to 290 °C. The desolvated phases of both compounds were obtained by heating the samples for 24 h at 100 °C under reduced pressure. The PXRD patterns of desolvated frameworks match well with the as-synthesized compounds and that indicates the stability of compounds **1** and **2** after removal of guest molecules (Fig. S18-S19).

Adsorption Studies

To evaluate the porosity and adsorption capacity of compounds **1** and **2**, we have carried out N$_2$ (kinetic diameter, 3.64 Å) and CO$_2$ (3.3 Å) gas adsorption measurements at low temperature.

Activated frameworks of **1** and **2** show very less uptake (1.8 cm^{3}g^{-1} in **1**, 7.3 cm^{3}g^{-1} in **2**) for N$_2$ at 77 K, although it is expected in case of **1** (from PLATON analysis) whereas in **2**, the framework contains comparable pore dimensions to permit the passage of N$_2$ (kinetic diameter, 3.64 Å) (Fig. 3). Such type of phenomenon is uncommon for microporous MOFs and the probable reason might be due to the presence of a 1D channel system in **2**, and no additional channels are available along the crystallographic *a*- and *c*-axes. Therefore, at low temperature (77 K) some nitrogen molecules interact very strongly with the pore aperture around the metal centers having polar environment, which block other nitrogen molecules from entering the pores as suggested by Kitagawa.[15]
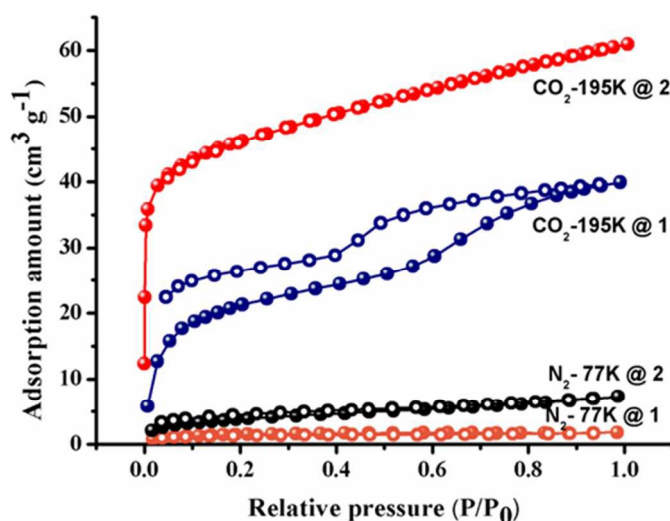
Fig. 3. Gas adsorption studies of **1** and **2** performed at low temperature.

The CO$_2$ adsorption isotherms of **1** and **2** measured at 195 K are shown in Fig. 3. Interestingly, compound **1** shows a two-step sorption isotherm. In step-1, which ranges from 0 to 0.55 bar, compound **1** adsorbs 27.14cm^{3}g^{-1} of CO$_2$ and at the second step, which ranges from 0.60 bar to 1 bar it adsorbs 39.19 cm^{3}g^{-1}, Whereas compound **2** shows type-I adsorption isotherm with the uptake amount of 60.9 cm^{3}g^{-1}. The observed two step sorption in case of **1** might be due to the breathing effect of framework as suggested by F´erey et al.,[16a] Zhou et al.,[16b] and several others.[16c,d]

Table.1 Virial graph analysis of compound **2**

Temperature (K)	adsorbate	$A_0 \ln(mol\ g^{-1}\ Pa^{-1})$	Henry's const K_H (mol g^{-1} Pa^{-1})	R^2	S_{ij}
273	CO_2	-15.19233	2.52×10^{-7}	0.99306	41
273	CH_4	-18.90889	6.13×10^{-9}	0.98914	
298	CO_2	-16.82833	4.91×10^{-8}	0.98905	19
298	CH_4	-19.8144	2.48×10^{-9}	0.98054	
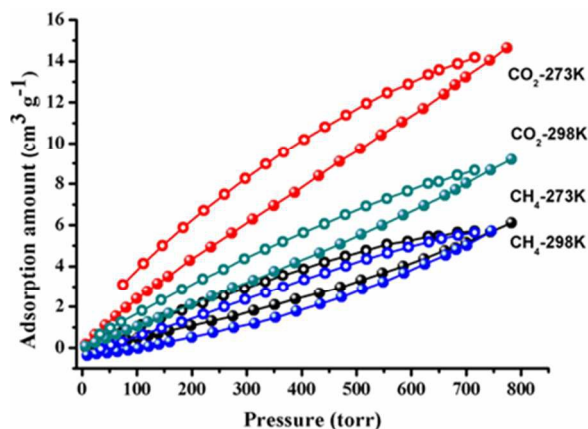
Fig. 4. Gas adsorption isotherms of compound **1** at around room temperature (273 and 298 K).
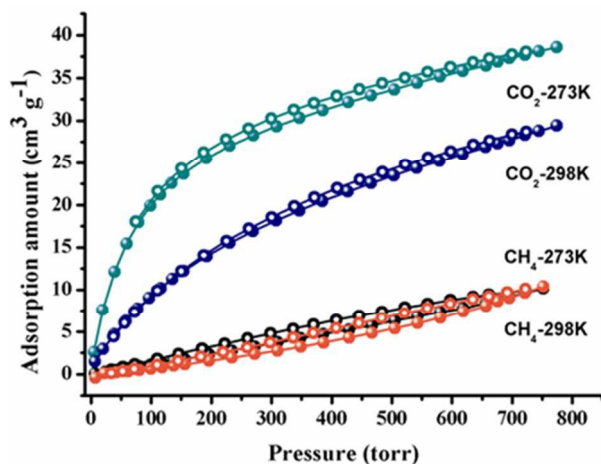
Fig. 5. Gas adsorption isotherms of compound **2** at around room temperature (273 and 298 K).

The selective uptake of CO_2 over N_2 in **1** and **2** could be due to the presence of V-shaped sdb linker and base functionalities (-C=N-N=C- group) in both 4-bpmh and 3-bpmh on the pore walls,[17] which can strongly interact with the quadruple moment $(-1.4 \times 10^{-35}\ C \cdot m)$[18] of CO_2 molecules respectively.

To get insight into the significant change in CO_2 uptake, we examined the structures of **1** and **2** carefully. Compounds **1** and **2** having same azine functional group (4-bpmh (**1**) and 3-bpmh(**2**)), V-shaped sdb linker, and same with an octahedral geometry of the Cd(II) ions and it is likely that the only difference in pore size and void space. Compound **1** has 2D interdigitated architectures and the voids obstruction because of

the role of 4-bpmh ligands whereas compound **2** is a 2-fold interwoven 3D porous network and hence it can interact with the CO_2 molecules effectively which consequently provides extra energy of adsorption over the compound **1**.

We have also carried out sorption experiments with CO_2 and CH_4 for **1** and **2** at 273 K and 298 K. The adsorption isotherms of CO_2 for compound **1** and **2** show a gradual increase and reach to the maximal amounts of 14.6 cm^3/g (2.8 wt%) and 38.2 cm^3/g (7.5 wt%) 273 K, 9.2 cm^3/g (1.8 wt%) and 29.2 cm^3/g (5.7 wt%) at 298 K respectively (Fig. 4 and 5). To further evaluate the interaction between the adsorbed CO_2 molecules and the host framework of **1** and **2**, isosteric heats (Q_{st}) of CO_2 adsorption are calculated based on the adsorption data collected at 273 K and 298 K by Clapeyron method.[19] The Q_{st} values at zero loading for **1** and **2** are -27.09 kJ mol^{-1} and -50.06 kJ mol^{-1} respectively (Fig. S20). Based on this observation we concluded that CO_2 interacts more strongly with compound **2** over **1**. In contrast, the capture capacities of **1** and **2** for CH_4 are extremely poorer (Fig. 4 and 5). The adsorption enthalpy of **1** and **2** for CH_4 at zero loading is approximately -21 kJ mol^{-1} and -11 kJ mol^{-1} respectively (Fig. S21). Based on this observation it can be concluded that CO_2 interacts more strongly than CH_4 with the framework due to the existence of a quadrupole moment for the former but not for CH_4.[20]

The enhancement in CO_2 uptakes found in compound **2** prompted us to investigate their CO_2 adsorption selectivity over CH_4. The adsorption selectivity of CO_2 over CH_4 was calculated for **2** by using the equation $S_{ij} = K_H(CO_2)/K_H(j)$ (Table 1 and Fig. S22) based on Henry's law.[21] The CO_2/CH_4 separation selectivity attained a value of 41 and 19 at 273 K and 298 K respectively. The observed selectivity value of **2** (~41) is well comparable with some reported MOF materials under similar conditions[22] (Table S1).

Furthermore, to check the structural stability of both frameworks after adsorption of CO_2 and CH_4, compounds were subjected to PXRD analysis. The PXRD patterns of CO_2 and CH_4 adsorbed samples match well with those of the as-synthesized samples (Fig. S23-24). This clearly indicates that the frameworks remain unchanged after adsorption CO_2 and CH_4.

Luminescence behaviors and sensing properties

To examine the luminescence properties of **1** and **2**, photoluminescence spectra of both compounds and their respective free ligands were recorded in solid state at room temperature.
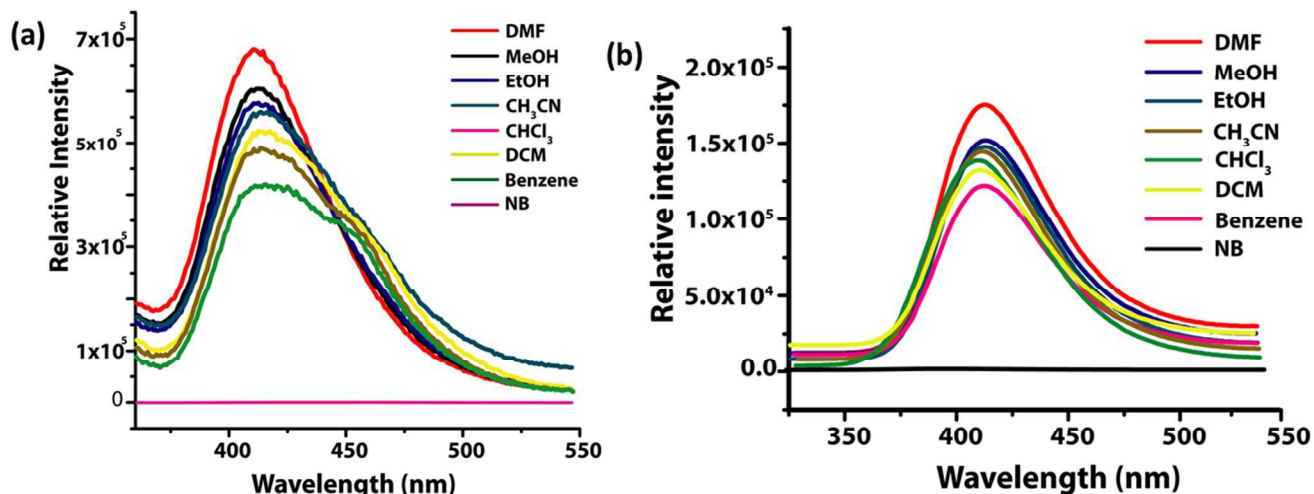
Fig. 6 Emission spectra of (a) compound **1** and (b) compound **2** in various solvents.
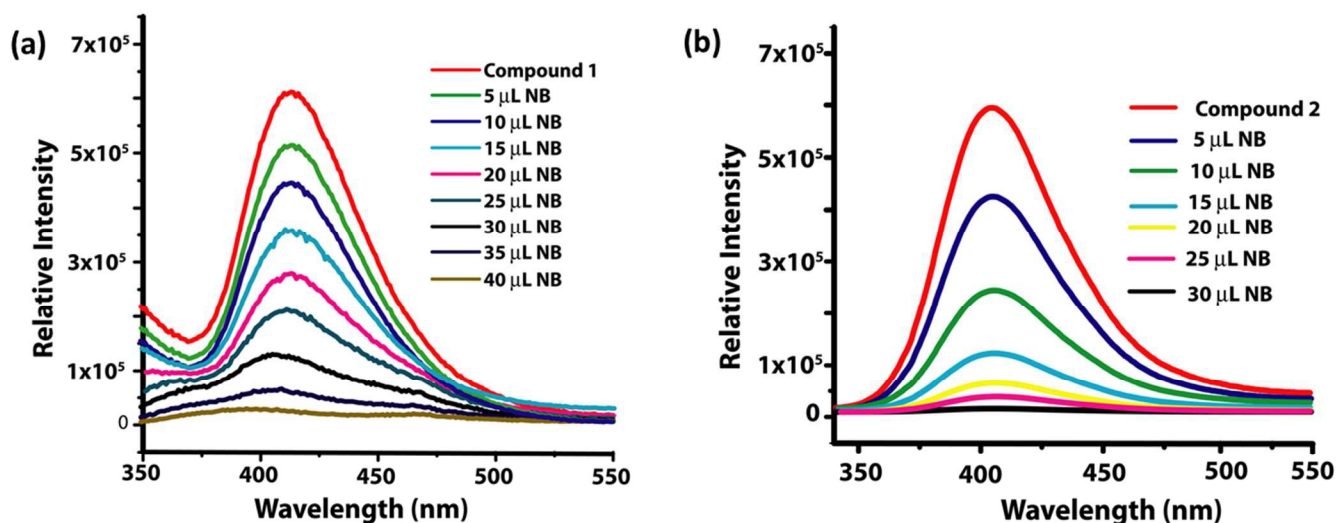

Fig. 7 Luminescent spectra of (a) **1** and (b) **2** in DMF with various amounts of nitrobenzene.

It was found that H$_2$sdb, 3-bpmh, and 4-bpmh ligands show stronger emissions at 323 nm (λ ex = 270 nm), 350 nm (λ ex = 243 nm), and 402 nm (λ ex = 231 nm), which can be attributed to $\pi^* \rightarrow \pi$ and/or $\pi^* \rightarrow$ n transitions (Fig. S25).[23] Both compounds display strong emissions at 412 nm upon excitation at 275 nm for **1** and 280 nm for **2**. The emission bands of **1** and **2** indicate significant red shifts, which can be attributed to the charge transfer from metal centers to ligands.[24]

To know the solvent effect on luminescence properties, emission spectra of **1** and **2** were investigated with suspensions in common solvents. Before every measurement, finely grounded samples (5 mg) of **1** and **2** were dispersed separately in 5 mL of different organic solvents, stirred for 24 h and then aged to form stable emulsions. The solvents used are *N,N*-dimethylformamide (DMF), ethanol, methanol, chloroform (CHCl$_3$), dichloromethane (CH$_2$Cl$_2$), acetonitrile, benzene and

nitrobenzene (NB). It was found that, the fluorescence intensities of **1** and **2** were almost unchanged upon addition of most of the analytes but in case of nitrobenzene a complete quenching effect was observed (Fig 6). Such solvent-dependent quenching behavior is of interest towards NB sensing and thus it was examined in more detail.

Fluorescence quenching titrations were performed with emulsions of **1** and **2** in DMF by the incremental addition of NB in DMF solutions (from 5 μL to 40 μL). As shown in Figure 7, the luminescence intensities are completely quenched upon addition of 40 ppm (98 %) and 30 ppm (99%) of NB respectively. The quenching efficiency is defined by $(I_0 - I)/I_0 \times 100\%$, where I_0 and I are the luminescence intensities of **1** and **2** before and after the addition of NB respectively. Quenching of the luminescence intensity and slight shifts in emission wavelengths of **1** and **2** upon the incremental addition

of NB might be due to the presence of electrostatic interaction between NB and the MOF.[25]

Moreover, both the compounds were recovered by centrifuging the dispersed solution of NB and the frameworks were found to remain intact, confirmed by PXRD patterns (Fig. S26 and S27). Remarkably, the initial fluorescence intensity was almost regained even after five cycles. The above observations clearly explain the potential of both compounds for sensing of NB and such a high sensitivity for nitrobenzene detection using an interpenetrating MOF has not been reported so far.[26]

It is well known that, nitro group is an electron withdrawing substituent and can stabilize the lowest unoccupied molecular orbital (LUMO) of aromatic products via conjugation compared with other solvents. Therefore, fluorescence sensing can be attributed to the photo-induced electron transfer from an excited MOF to the electron deficient NB adsorbed on the surface of the MOF through interspecies contacts (which might lead to electron transfer).[27]

Conclusion

In conclusion, we have synthesized two metal−organic frameworks (MOFs) by changing the coordination positon of nitrogen through ligand modification. Gas adsorption studies demonstrate that compound **2** shows high selectivity for CO_2 over CH_4 and the uptake amounts are almost double in comparison with compound **1**. The emulsions of both compounds exhibit a strong emission which could be quenched in presence of trace amounts of nitrobenzene, revealing that the current materials can be potentially useful for detecting poisonous substances.

EXPERIMENTAL SECTION

Materials and Methods

All the reagents and solvents for synthesis were purchased from commercial sources and used as supplied without further purification. $Cd(NO_3)_2 \cdot 4H_2O$, 4,4'-Sulfonyl dibenzoic acid, 4-Pyridine aldehyde and 3-Pyridine aldehyde were obtained from the Sigma-Aldrich Chemical Co. India. 4-bpmh and 3-bpmh were synthesized by the literature procedure.[28] The elemental analyses were carried out on Elementar micro vario cube elemental analyser. FT-IR spectra (4000 – 500 cm^{-1}) were recorded on a KBr pellet with a Perkin Elmer Spectrum BX spectrometer. Powder X-ray diffraction (PXRD) data were collected on a PANalytical EMPYREAN instrument using Cu-Kα radiation. Absorption and emission spectra were recorded using a Carry 100 UV-vis spectrophotometer (Agilent technologies).

Fluorescence experiments

All the solid and liquid state fluorescence measurements were recorded on Horiba Jobin-Yvon Fluorolog3 instrument. For a typical experimental setup in liquid state, in a 1 cm quartz cuvette, 3 mL solutions of compounds **1** and **2** in DMF were placed separately and the fluorescence response upon

respective excitation was measured in-situ in the range of 320-550 nm after incremental addition of freshly prepared analyte solutions (while keeping 4 nm slit width for both the source and the detector). To maintain homogeneity, solution was stirred at constant rate during experiment.

Table 2. Crystallographic refinement parameters for compounds **1** and **2**.

Complex	1	2
CCDC	1433199	1024644
Formula	$C_{51}H_{40}Cd_2N_9O_{15}S_2$	$C_{58}H_{47}Cd_2N_9O_{16}S_2$
Formula weight (g/M)	1307.86	1414.99
Crystal shape	Block	Block
Color	Yellow	Yellow
T (K)	296(2)	296(2)
Wavelength(Å)	0.71073	0.71073
Space group	*P* -1	*P* 2/n
Crystal system	Triclinic	Monoclinic
a/ Å	14.735(3)	13.0797
b/ Å	15.297(2)	25.5407
c/ Å	15.798(2)	19.3452
α/deg	114.043	90
β/deg	96.162	104.73
γ/deg	116.120	90
V/Å^3	2735.5	6250.1
Z	2	4
D$_{calcd}$ (g cm^{-3})	1.542	1.332
μ(mm^{-1})	0.922	0.806
F(000)	1276	2512.0
Reflection Collected	9903	11163
Unique Reflections	6136	7095
GOOF	1.032	0.890
^{a}R1	0.0879	0.0381
^{b}wR2(I>2σ(I))	0.2301	0.0705

^{a}R1 = Σ||Fo| - |Fc||/Σ|Fo|, ^{b}wR2 = [Σw(Fo^2- Fc^2)/(Fo^2)2]$^{1/2}$

Single crystal X-ray diffraction

Single crystal data for compound **1** and **2** were collected on a Bruker APEX II diffractometer equipped with a graphite monochromator and Mo-Kα (λ = 0.71073 Å, 296 K) radiation. Data collections were performed using φ and ω scan. Non-hydrogen atoms located from the difference Fourier maps, were refined anisotropically by full-matrix least-squares on F^2, using SHELXS-97.[29] All hydrogen atoms were included in the calculated positions and refined isotropically using a riding model. Determinations of the crystal system, orientation matrix, and cell dimensions were performed according to the established procedures. Lorentz polarization and multi-scan absorption correction were applied. All calculations were carried out using SHELXL 97,[30] PLATON 99,[13] and WinGXsystemVer-1.64.[31] In compound **1**, a few carbon atoms in the main fragments bear thermal disorder and the disorder treatment has been carried out with DELU and DFIX command. In compound **1** and **2,** during the final stages of refinement, some Q peaks having high electron densities were found, which corresponding to solvent molecules are too disordered to assign and hence are squeezed out using SQUEEZ program in PLATON. Compound **2** bears a thermally disordered 3-Pyridinecarboxaldehyde, which is used in the synthesis of 3-bpmh ligand and hence is squeezed out using SQUEEZ program in PLATON. From the TG analysis, we have calculated that in compound **1**, two guest H_2O molecules

are present, whereas in **2** one 3-pyridinecarboxaldehyde and three H_2O molecules are present, and hence those are included in the molecular formula. Data collection, structure refinement parameters and crystallographic data are given in Table **2** and selected bond lengths and bond angles for compounds **1** and **2** are given Table S2-S3.

Sorption measurements

Gas adsorption measurements were performed by using BelSorp-max (BEL Japan) automatic volumetric adsorption instrument. All the gases used were ultra-pure research grade (99.99%). Before every measurement samples were pre-treated for 12h at 423 K under 10^{-2}KPa continuous vacuum using BelPrepvac II and purged with N_2 on cooling. CO_2 isotherms were measured at 195 K by using dry ice-MeOH cold bath and also recorded at 273 K by using Julabo chiller with Ethylene glycol-water mixture as a coolant.

Virial graph analysis.

Virial Model[20] provides a general method of analyzing the low coverage region of an adsorption isotherm and its application is not restricted to particular mechanisms or systems (equation 1).

$$p = n\, exp(C_1 + C_2 n + C_3 n^2 + ..)\ \ \ \ \ .....\ (1)$$

where the coefficients (C_1, C_2, C_3) are characteristic constants for a given gas-solid system and temperature. The linear form of the equation 2 is:

$$\ln\left(\frac{n}{p}\right) = K_0 + K_1 n + K_2 n^2 + ..\ \ \ ....\ (2)$$

Where p is pressure, n is the amount adsorbed, and K_0, K_1, etc., are virial coefficients. K_0 is related to adsorbate-adsorbent interactions, whereas K_1 describes adsorbate-adsorbate interactions.

Thus the intercept of the virial plot of ln (n/p) versus n, it is possible to obtain Henry's constant, k_H, since (equation 3)

$$K_H = \lim_{n \to \infty}\left(\frac{n}{p}\right)\ \ \ \ ....\ (3)$$

Therefore, K_1 is directly related to k_H and to the gas-solid interaction.

Henry's constants determined from the Virial plot of ln (p/n) vs n are also presented and they indicate the the interaction parameter of the gas molecule with the adsorbent surface and the selectivity for CO_2 (i) over different gases (j) calculated as $S_{ij} = K_H(CO_2)/K_H(j)$.

Synthesis of $\{[Cd_2(sdb)_2(4\text{-bpmh})_2(H_2O)]\}_n \cdot 2n(H_2O)$ (1):

An aqueous solution (20 mL) of Na_2sdb (1 mmol, 310 mg) was mixed with methanol solution (20 mL) of 4-bpmh (1 mmol, 210 mg) and the resulting solution was stirred for 1h to mix well. $Cd(NO_3)_2\cdot4H_2O$ (1 mmol, 311 mg) was dissolved in 20 mL of water in a separate beaker. 3 mL of the above mixed ligand solution was slowly and carefully layered above 3 mL of metal solution in a narrow glass tube using 2 mL of buffer solution

(1:1 H_2O and MeOH). X-ray quality yellow-colored block-shaped single crystals were obtained from the junction of the layer after 14 days. The crystals were separated and washed with methanol and air-dried. Elemental analysis: Cald. for $C_{51}H_{40}Cd_2N_9O_{15}S_2$ (%). C, 46.8; N, 9.6; S, 4.9; H, 3.08; Found (%): C, 47.5; N, 8.3; S, 5.2; H, 2.7; **FT-IR** (KBr pellet, cm^{-1}): 3444 (b), 1622 (s), 1568 (s), 1400 (s), 1072 (m), 830 (w), 785 (w), 533 (w).

Synthesis of $\{[Cd_2(sdb)_2(3\text{-bpmh})_2]\}_n \cdot 3n(H_2O)\cdot n(C_6H_5NO)$:

An aqueous solution (20 mL) of Na_2sdb (1 mmol, 310 mg) was mixed with methanol solution (20 mL) of 3-bpmh (1 mmol, 210 mg) and the resulting solution was stirred for 1h to mix well. $Cd(NO_3)_2\cdot4H_2O$ (1 mmol, 311 mg) was dissolved in 20 mL of water in a separate beaker. 3 mL of the above mixed ligand solution was slowly and carefully layered above 3 mL of metal solution in a narrow glass tube using 2 mL of buffer solution (1:1 H_2O and MeOH). X-ray quality yellow-colored block-shaped single crystals were obtained from the junction of the layer after 3 days. The crystals were separated and washed with methanol and air-dried. Elemental analysis: Cald. for $C_{58}H_{47}Cd_2N_9O_{16}S_2$ (%). C, 49.2; N, 8.9; S, 4.5; H, 3.3; Found (%): C, 50.1; N, 8.2; S, 4.9; H, 2.7; **FT-IR** (KBr pellet, cm^{-1}): 3428 (b), 1630 (s), 1420 (s), 1386 (s), 1308 (w), 1233 (m), 1191 (s), 1116 (b), 1028 (m), 958 (m), 798 (s), 697 (s).

Author Contributions

‡ These authors contributed equally to this work.

† Undergraduate researcher

Notes and References

1. K. S. Lackner, S. Brennan, J. M. Matter, A. -H. A. Park, A. Wright and B. van der Zwaan, *Proc. Natl. Acad. Sci. U. S. A.*, 2012, **109**, 13156.

2. (a) H. Furukawa and O. M. Yaghi, *J. Am. Chem. Soc.*, 2009, **131**, 8875; (b) J. Lan, D. Cao, W. Wang and B. Smit, *ACS Nano.*, 2010, **4**, 4225.

3. (a) K. S. Park, N. Zheng, A.-P. Côté, J. Y. Choi, R. Huang, F. J. Uribe-Romo, H. K. Chae, M. O'Keeffe and O. M. Yaghi, *Proc. Natl. Acad. Sci. U. S. A.,* 2006, **103**, 10186; (b) X.-C. Huang, Y.-Y. Lin, J.-P. Zhang and X.-M. Chen, *Angew. Chem., Int. Ed.,* 2006, **45**, 1557.

4. (a) O. K. Farha, I. Eryazici, N. C. Jeong, B. G. Hauser, C. W. Wilmer, A. A. Sarjeant, R. Q. Snurr, S. T. Nguyen, A. O. Yazaydın and J. T. Hupp, *J. Am. Chem. Soc.*, 2012, **134**, 15016; (b) T. Uemura, N. Yanaia and S. Kitagawa, *Chem. Soc. Rev.,* 2009, **38**, 1228; (c) J. C. Kepert, *Chem. Commun.*, 2006, 695; (d) Schroder, M. *Springer.*,

Berlin, 2010. d) O. K. Farha, I. Eryazici, N. C. Jeong, B. G. Hauser, C. E. Wilmer, A. A. Sarjeant, R. Q. Snurr, S. T. Nguyen, A. O. Yazaydın and J. T. Hupp, *J. Am. Chem. Soc.,* 2012, **134**, 15016;

5. (a) M. Kandiah, M. H. Nilsen, S. Usseglio, S. Jakobsen, U. Olsbye, M. Tilset, C. Larabi, E. A. Quadrelli, F. Bonino and K. P. Lillerud, *Chem. Mater.,* 2010, **22**, 6632; (b) M. L. Foo, S. Horike, T. Fukushima, Y. Hijikata, Y. Kubota, M. Takata and S. Kitagawa, *Dalton Trans.,* 2012, **41**, 13791.

6. (a) S. J. Toal and W. C. Trogler, *J. Mater. Chem.,* 2006, **16**, 2871; (b) M. E. Germain and M. J. Knapp, *Chem. Soc. Rev.,* 2009, **38**, 2543; (c) K. D. Smith, B. R. McCord, W. A. MacCrehan, K. Mount and W. F. Rowe, *J. Forensic Sci.,* 1999, **44**, 789; (d) D. T. McQuade, A. E. Pullen and T. M. Swager, *Chem. Rev.,* 2000, **100**, 2537.

7. (a) S. A. Boyd, G. Sheng, B. J. Teppen and C. T. Johnston, *Environ. Sci. Technol.,* 2001, **35**, 4227; (b) M. T. Cronin, B. W. Gregory and T. W. Schultz, *Chem. Res. Toxicol.,* 1998, **11**, 902; (c) P. S. Majumder and S. K. Gupta, *Water Res.,* 2003, **37**, 4331.

8. (a) A. W. Czarnik, *Nature.,* 1998, **394**, 417; (b) D. S. Moore, *Rev. Sci. Instrum.,* 2004, **75**, 2499; (c) S. A. McLuckey, D. E. Goeringer, K. G. Asano, G. Vaidyanathan and J. L. Stephenson Jr, *Rapid Commun. Mass Spectrom.,* 1996, **10**, 287.

9. (a) A. K. Chaudhari, S. S. Nagarkar, B. Joarder and S. K. Ghosh, *Cryst. Growth Des.,* 2013, **13**, 3716; (b) T. Naddo, Y. Che, W. Zhang, K. Balakrishnan, X. Yang, M. Yen, J. Zhao, J. S. Moore and L. Zang, *J. Am. Chem. Soc.,* 2007, **129**, 6978; (c) D.-X. Ma, B.-Y. Li, X.-J. Zhou, Q. Zhou, K. Liu, G. Zeng, G.-H. Li, Z. Shi and S.-H. Feng, *Chem. Commun.,* 2013, **49**, 8964. (d) S. Sanda, S. Parshamoni, S. Biswas and S. Konar, *Chem. Commun.,* 2015, **51**, 6576; (e) Z. Hu, B. J. Deibert and J. Li, *Chem. Soc. Rev.,* 2014, 43, 5815; (f) Y. Cui, Y. Yue, G. Qian and B. Chen, *Chem. Rev.,* 2012, 112, 1126. (g) S. S. Nagarkar, B. Joarder, A. K. Chaudhari, S. Mukherjee and S. K. Ghosh, *Angew. Chem., Int. Ed.,* 2013, **52**, 2881; (h) B. Gole, A. K. Bar and P. S. Mukherjee, *Chem. – Eur. J.,* 2014, **20**, 2276.

10. (a) S. Parshamoni, S. Sanda, H. S. Jena, K. Tomar and S. Konar, *Cryst. Growth Des.,* 2014, **14**, 2022; (b) A. Jalal, S. Shahzadi, K. Shahid, *Turk. J. Chem.,* 2004, **28**, 629.

11. (a) R. A. Coxall, S. G. Harris, D. K. Henderson, S. Parsons, P. A. Tasker and R. E. P. Winpenny, *J. Chem. Soc. Dalton Trans.* 2000, 2349; (b) S. Khatua, S. Goswami, S. Parshamoni, H. S. Jena and S. Konar, *RSC Adv.,* 2013, **3**, 25237.

12. V. A. Blatov, A. P. Shevchenko, V. N. Serezhkin, TOPOS3.2: a new version of the program package for multipurpose crystal− chemical analysis. *J. Appl. Crystallogr.,* 2000, **33**, 1193.

13. A. L. Spek, *J. Appl. Crystallogr.,* 2003, **36**, 7.

14. (a) V. A. Blatov, A. P. Shevchenko and V. N. J. Serezhkin, *J. Appl. Crystallogr.,* 2000, **33**, 1193; (b) V. A. Blatov, L. Carlucci, G. Ciani and D. M. Proserpio, *CrystEngComm.,* 2004, **6**, 378; (c) A. V. Blatov and D. M. Proserpio, *Acta Crystallogr., Sect. A: Found. Crystallogr.,* 2009, **65**, 202.

15. (a) T. K. Maji, R. Matsuda and S. Kitagawa, *Nat. Mater.,* 2007, **6**, 142; (b) M. Du, C. P. Li, M. Chen, Z. W. Ge, X. Wang, L. Wang and C. Liu, *J. Am. Chem. Soc.,* 2014, **136**, 10906; (c) S. Parshamoni, S. Sanda, H. S. Jena and S. Konar, *Dalton Trans.,* 2014, **43**, 7191; (d) S. Parshamoni, H. S. Jena, S. Sanda and S. Konar, *Inorg. Chem. Front.,* 2014, **1**, 611; (e) S. Sanda, S. Parshamoni and S. Konar, *Inorg. Chem.,* 2013, **52**, 12866.

16. (a) N. A. Ramsahye, G. Maurin, S. Bourrelly, P. L. Llewellyn, T. Loiseau, C. Serre, and G. Fe´rey, *Chem. Commun.,* 2007, 326; (b) D. Yuan, R. B. Getman, Z. Wei, R. Q. Snurr and H. -C. Zhou, *Chem. Commun.,* 2012, **48**, 3297; (c) N. Nijem, H. Wu, P. Canepa, A. Marti, K. J. Balkus, T. Jr. Thonhauser, J. Li and Y. J. Chabal, *J. Am. Chem. Soc.,* 2012, **134**, 15201; (d) T. −F. Liu, J. Lü, and R. Cao, *CrystEngComm.,* 2010, **12**, 660.

17. (a) R. Dey, B. Bhattacharya, E. Colacio and D. Ghoshal, *Dalton Trans.,* 2013, **42**, 2094; (b) C. M. Nagaraja, R. Haldar, T. K. Maji and C. N. R. Rao, *Cryst. Growth Des.,* 2012, **12**, 975; (c) S Parshamoni, S Sanda, H. S. Jena, and S. Konar, *Chem. Asian J.,* 2015, **10**, 653.

18. (a) S. Bourrelly, P. L. Llewellyn, C. Serre, F. Millange, T. Loiseau and G. Ferey, *J. Am. Chem. Soc.,* 2005, **127**, 13519; (b) P. L. Llewellyn, S. Bourrelly, C. Serre, Y. Filinchuk and G. Férey, *Angew. Chem., Int. Ed.,* 2006, **45**, 7751; (c) K. S. Walton, A. R. Millward, D. Dubbeldam, H. Frost, J. J. Low, O. M. Yaghi and R. Q. Snurr, *J. Am. Chem. Soc.,* 2008, **130**, 406; (d) P. K. Thallapally, B. P. McGrail, S. J. Dalgarno, H. T. Schaef, J. Tian and J. L. Atwood, *Nat. Mater.,* 2008, **7**, 146. (e) S. Goswami, S. Sanda and S. Konar, *CrystEngComm.,* 2014, **16**, 369; (f) H. S. Jena, S. Goswami, S. Sanda, S. Parshamoni, S. Biswas and S. Konar, *Dalton Trans.,* 2014, **43**, 16996.

19. J. J. Perry IV, V. Ch. Kravtsov, G. J. McManus and M. J. Zaworotko, *J. Am. Chem. Soc.,* 2007, **129**, 10076.

20. S. S. Nagarkar, A. K. Chaudhari and S. K. Ghosh, *Inorg. Chem.,* 2012, **51**, 572.

21. Z. Chen, S. Xiang, H. D. Arman, J. U. Mondal, P. Li, D. Zhao and B. Chen, *Inorg. Chem.,* 2011, **50**, 3442.

22. (a) B. Zheng, Z. Yang, J. Bai, Y. Li and S. Li, *Chem. Commun.,* 2012, **48**, 7025; (b) B. Mu, F. Li and K. S. Walton, *Chem. Commun.,* 2009, 2493; (c) L. Du, Z. Lu, K. Zheng, J. Wang, X. Zheng, Y. Pan, X. You, and J. Bai, *J. Am. Chem. Soc.,* 2013, **135**, 562; (d) Car, C. Stropnik, K.-V. Peinemann, *Desalination.* 2006, **200**, 424; (e) Y. F. Zhang, I. H. Musseman, J. P. Ferraris and K. J. Balkus, *J. Membr. Sci.,* 2008, **313**, 170; (f) S. Basu, A. Cano-Odena and I. F. J. Vankelecom, *J. Membr. Sci.,* 2010, **362**, 478; (h) R. Banerjee, H. Furukawa, D. Britt, C. Knobler, M. O'Keeffe and O. M. Yaghi, *J. Am. Chem. Soc.,* 2009, **131**, 3875.

23. (a) W. Yang, F. Yi, X. Li, L. Wang, S. Dang and Z. Sun, *RSC Adv.,* 2013, **3**, 25065; (b) H. Wang, F. Yi, S. Dang, W. Tian and Z. Sun, *Cryst. Growth Des.,* 2014, **14**, 147; (c) R. B. Fu, S. C. Xiang, S. M. Hu, L. S. Wang, Y. M. Li, X. H. Huang and X. T. Wu, *Chem. Commun.,* 2005, 5292; (d) Y. Rachuri, K. K. Bisht, and E. Suresh, *Cryst. Growth Des.,* 2014, **14**, 3300.

24. (a) M. D. Allendorf, C. A. Bauer, R. K. Bhakta, R. J. T. Houk, *Chem. Soc. Rev.,* 2009, **38**, 1330; (b) D. P. Martin, M. A. Braverman, R. L. LaDuca, *Cryst. Growth Des.,* 2007, **7**, 2609.

25. (a) Y. Rachuri, B. Parmar, K. K. Bisht and E. Suresh, *Inorg. Chem. Front.,* 2015, **2**, 228; (b) S. S. Nagarkar, A. V. Desai and S. K. Ghosh, *Chem. Commun.,* 2014, **50**, 8915; (b) Y.-N. Gong, Y.-L. Huang, L. Jiang and T.-B. Lu, *Inorg. Chem.,* 2014, **53**, 9457.

26. (a) Y. Kim, J. H. Song, W. R. Lee, W. J. Phang, K. S. Lim and C. S. Hong, *Cryst. Growth Des.,* 2014, **14**, 1933; (b) D. Tian, Y. Li, R. Y. Chen, Z. Chang, G. Y. Wang and X. H. Bu, *J. Mater. Chem. A.,* 2014, **2**, 1465.

27. (a) G. Y. Wang, L. L. Yang, Y. Li, H. Song, W. J. Ruan, Z. Chang and X. H. Bu, *Dalton Trans.,* 2013, **42**, 12865; (b) H. Sohn, M. J. Sailor, D. Magde and W. C. Trogler, *J. Am. Chem. Soc.,* 2003, **125**, 3821.

28. (a) A. R. Kennedy, K. G. Brown, D. Graham, J. B. Kirkhouse, M. Kittner, C. Major, C. J. McHugh, P. Murdoch and W. E. Smith, *New J. Chem.*, 2005, **29**, 826; (b) S. Sanda, S. Parshamoni, A. Adhikary and S. Konar, *Cryst. Growth Des.*, 2013, **13**, 5442.

29. G. M. Sheldrick, SHELXTL Program for the Solution of Crystal of Structures, University of Göttingen, Göttingen, Germany, 1993.

30. (a) G. M. Sheldrick, SHELXL 97, Program for Crystal Structure Refinement, University of Göttingen, Göttingen, Germany, 1997 (b) O. V. Dolomanov, L. J. Bourhis, R. J. Gildea, J. A. K. Howard, H. Puschmann, OLEX2: A complete structure solution, refinement and analysis program. *J. Appl. Cryst.*, 2009, **42**, 339.

31. L. J. Farrugia, *J. Appl. Crystallogr.*, 1999, **32**, 837.

Table of Contents
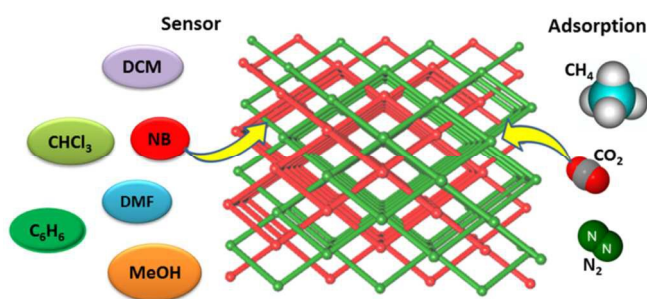
Two MOF's were constructed using azine functionalized and pyridyl based nutral ligands along with a V-shaped sdb linker, which exhibits highly efficient luminescence sensing for nitrobenze and sorption selectivity of CO_2 over CH_4.